Coupling between progressive damage and permeability of concrete: analysis with a discrete model

Georges Chatzigeorgiou, Vincent Picandet, Abdelhafid Khelidj, Gilles Pijaudier-Cabot

Coupling between progressive damage and permeability of concrete: analysis with a discrete model

George Chatzigeorgiou[1], Vincent Picandet[2], Abdelhafid Khelidj[3] and Gilles Pijaudier-Cabot[4]

[1] *Department of Civil Engineering, Division of Structures, University Campus, Aristotle University of Thessaloniki, 54006 Thessaloniki, Greece*

[2] *LG2M, Université de Bretagne Sud, Rue de Saint Maudé, BP 92116, 56321 Lorient Cedex, France*

[3] *R&DO, Institut GeM/UMR CNRS 6183, I.U.T. de Saint Nazaire, dépt. Génie Civil, BP 420 Heinlex, 44600 Saint-Nazaire, France*

[4] *R&DO, Institut GeM/UMR CNRS 6183, Ecole Centrale de Nantes, 1 rue de la Noë, BP 92101, F44321 Nantes Cedex 3, France*

A significant increase of the permeability of concrete upon micro-cracking and a good correlation between the evolution of damage (material stiffness) and permeability are observed experimentally. The present contribution investigates this correlation theoretically, with the help of lattice analyses. Scaling analysis of lattices which contain elastic brittle bonds has shown that the material degradation should be described by the evolution of the material stiffness, or compliance, in a continuum setting (damage models). This result is reviewed and further documented in the first part of the paper. In the second part, hydro-mechanical problems are considered with the construction of a hydraulic lattice, dual to the mechanical one. We observe that the average permeability upon micro-cracking is the lattice scale-independent controlling variable in the hydraulic problem. Additionally, results show that in a continuum poro-mechanical approach, the evolution of the material permeability ought to be related to the elastic unloading stiffness, described e.g. with the help of continuum damage variables.

KEY WORDS: damage; discrete model; permeability

1. INTRODUCTION

In large structures such as concrete nuclear vessels where the long-term safety is of high priority, durability is important for design. Among the parameters playing a pivotal role, material permeability is one of the most important if one considers that vessels should not exhibit a

leakage rate above a certain threshold whenever there is a sudden increase of pressure inside the vessel (for instance due to integrity tests). In most cases, apart from extremely severe accidents, mechanical loads induced by the increase of gas pressure inside the vessel yield moderate micro-cracking that can be viewed as distributed damage. Therefore, simulations of such case studies, with the aim of estimating the increase of leakage rate that is induced by internal pressure in vessels, ought to rely on material models in which the evolution of material permeability is related to the non-linear mechanical response of concrete.

In tension or compression (and for moderate confining pressures), concrete fails due to micro-crack propagation and coalescence. Micro-cracks, whose development at the beginning is almost homogeneous, start to concentrate in a region inside the material as the peak load is approached. Failure occurs with a sudden propagation of one or more macro-cracks. With the increase of cracking there is also a decrease in the stiffness of the material. In damage models, this reduction of stiffness is expressed through a damage parameter (see e.g. References [1, 2]).

Experimental results have shown that for low and intermediate stress levels (diffuse distribution of damage), the permeability of concrete to water [3, 4] or gas [5] exhibits a slow increase (typically of one order of magnitude at the most), and then increases dramatically by several orders of magnitude when the load is very close to the ultimate strength of the material and further in the softening regime. From a microscopic point of view, in the first regime up to the peak load [6], the width of the cracks is relatively small. Micro-cracks do not form a connected network. In the second regime, a macro-crack forms and the transfer properties of the structure become almost solely governed by the macro-crack opening and tortuosity (the permeability of the surrounding material is so small that its effect is negligible). In this contribution, we are interested in the first regime of relatively slow growth of permeability, as major through macro-cracks are not expected to occur in vessels under service conditions. Therefore, we look at modelling the relationship between micro-cracking and permeability in a material that can still be viewed as a continuum with a homogeneous (or slowly varying) distribution of micro-cracks.

Coupling between the non-linear response of concrete and its permeability can be achieved in a very standard way with the help of the theory of porous materials initially due to Biot (see e.g. References [7, 8]). This approach has become very popular in the literature for durability analyses involving mass transfer such as hydro-mechanical damage analyses [9], analysis of concrete at an early age [10], chemo-mechanical effects [11], and more generally environmentally induced degradations [12]. In these approaches, however, the relationship between the material permeability and the degradation induced in the material due to mechanical loads is phenomenological. Theoretical investigations of such relationships are relatively recent in the context of concrete materials. They are based on homogenization techniques [13, 14] where the distribution of micro-cracks needs to be characterized accurately (size, shape, opening, orientation). Such approaches provide a justification of the expected relationship between the crack density and the permeability. The applied effective stress may also play a role as far as the propagation of these micro-cracks is concerned.

Another approach, which serves the same purpose as homogenization techniques, is the scaling analysis of discrete lattices. Simple discrete models were used in the past in order to study the failure of heterogeneous materials. Two-dimensional lattice models consisting of beams [15] or springs [16] have been used, where the heterogeneity is captured by a random distribution of the failure thresholds of each beam/bar. Although these lattices are very simple, and not capable of reproducing the exact features of the micro-cracking processes in brittle heterogeneous

materials, the limit of a lattice of infinite size is related to the response of a material point in the continuum sense. Hence, there is an interest at studying the scaling properties of such lattices, and in particular the characteristics that describe the lattice in a size-independent way. Such quantities are those that are expected to be found in a continuum model, as representatives of the material degradation. Following this technique, Delaplace *et al.* [17] have shown that a proper way to capture material damage due to micro-cracking, described as the failure of elastic brittle bonds in a discrete model, is to model the variation of the material stiffness in a continuum setting (which can then be indexed by a damage variable). A similar observation has been also reported by Krajcinovic and Basista [18].

In this paper, we attempt the same type of approach with the aim of investigating the variation of material permeability due to mechanical damage and their relationship. We start with the mechanical analysis. We recall the main features of the study performed by Delaplace *et al.* [17], extending the analysis to lattices of larger sizes with a more representative statistical analysis. Hydro-mechanical coupling is then performed by superimposing two lattices: one for the mechanical problem and a second one for the hydraulic problem. We find that the hydraulic problem is described by the overall variation of stiffness observed in the mechanical problem. Therefore, the permeability of the unloaded material should indeed be correlated to continuum damage (and not to the applied stress history for instance). Finally, we compare the results with experimental curves obtained by Picandet *et al.* [19] from a qualitative point of view.

2. MECHANICAL PROBLEM

The lattice which will be described in the following was used in the past for the study of the failure mechanism of quasi-brittle materials (see [17, 20] for complete details). It is a stiffness-controlled model, where the mechanical problem is substituted by an electrical analogous, simplifying the analysis by transforming it from vectorial to scalar. As shown by De Arcangelis *et al.* [21], this simplification is able to capture the most important physical aspects of the problem with a simpler approach. The model, which is depicted in Figure 1(a), is a regular two-dimensional lattice whose bonds are one-dimensional. The lattice size is $L \times L$, where L is related to the total number of bonds $n = 2L^2$. Instead of solving the mechanical problem, we solve an electrical analogous substituting the strain ε with the voltage difference v, the stress σ with the current i, and the Young's Modulus E with the conductance G. So, we substitute the constitutive equation

$$\sigma = E \cdot \varepsilon \tag{1}$$

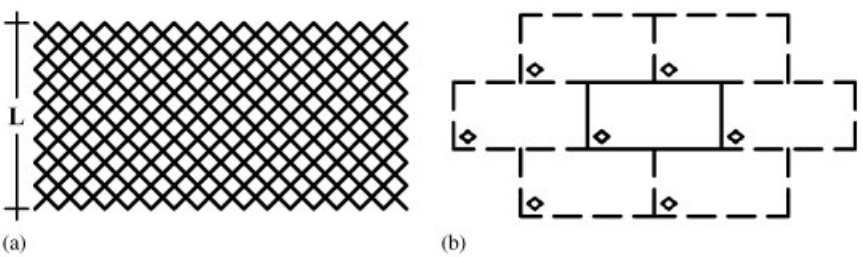

Figure 1. (a) Lattice model; and (b) the lattice in the infinity body with periodic boundary conditions.

with

$$i = G \cdot v \tag{2}$$

The boundary conditions of the model are periodic in order to attain the creation of an infinite system and to avoid boundary effects (Figure 1(b)). They represent a homogeneous loading in the vertical direction: periodicity is imposed along the boundaries parallel to the vertical axis and a constant unit jump of voltage is applied between the horizontal boundaries.

Every bond of the lattice behaves as a brittle material which has a conductance equal to 1. When it reaches a threshold current i_c, it fails (Figure 2). i_c differs from bond to bond following a uniform random distribution between 0 and 1.

We start the calculation by assigning a threshold current to every bond with the help of a random generator number [22]. At each step, the algorithm computes the voltage at each node from Kirchhoff's law. The equations form a symmetric band matrix which is solved using Cholesky factorization. From Ohm's law, the current of each bond is obtained. The bond which fails first is the one which has the minimum ratio of its strength i_c to its current. This bond is removed from the lattice by changing its conductance from 1 to 0. Because the analysis is linear, it is also possible to compute the overall load (intensity) at which this bond fails and the process continues with the next step of loading where we look at the next bond which fails. Figure 3 shows a typical current vs voltage response (lattice of size 64), and Figure 4 shows the lattice just before collapse (each broken bond corresponds to a small black line). The snapbacks in Figure 3 are observed because the load process is stiffness controlled. In a displacement-controlled scheme, the envelope of the curve would be recovered only. We can notice in Figure 4(a) that just before the complete collapse of the lattice, there is a large crack and a tremendous number of micro-cracks spread all over the material. The reason for this diffusion of the damage is the initial disorder in the lattice, a uniform distribution of the bond thresholds. With a narrow (Dirac delta) distribution, a single crack would propagate same as in a brittle material. If we recall that there are periodic boundary conditions on the lattice faces, we see in Figure 4(b), where the lattice is periodically repeated, that the macro-cracks inside the material are parallel lines whose distance is equal to the size of the lattice. This indicates the strong dependence of the lattice geometry in the final post-peak regime, which may not be considered for the scaling analyses aiming at a continuum description. The final macro-crack spacing is directly connected to the lattice size.

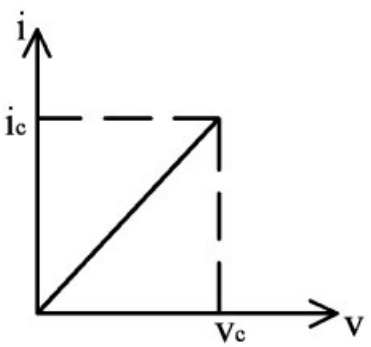

Figure 2. Current–voltage curve of a bond. The bonds have a unit resistance.

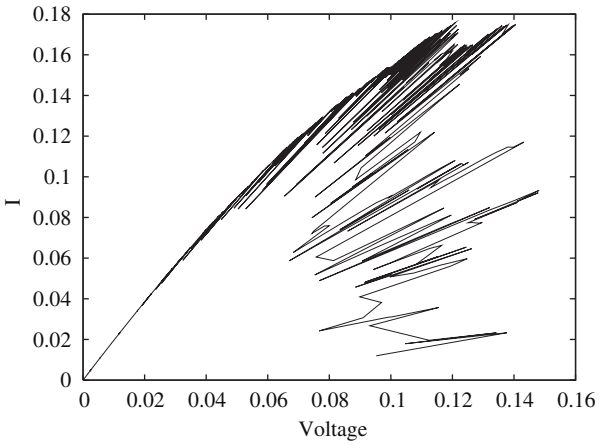

Figure 3. Typical intensity (load) versus voltage (relative displacement) response of a lattice of size 64.

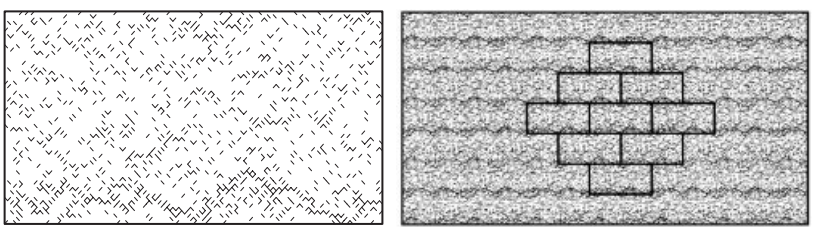

Figure 4. Lattice of size 64 just before collapse: (a) single cell; and (b) lattice cell duplicated according to the periodic boundary conditions.

The lattice does not represent a real material. In fact, we are interested in its scaling properties: as the lattice size tends to infinity, its response tends to a (thermodynamic) limit which is the response of a single point in a continuum approach. Hence, we shall look at the variables that are capable to describe the evolution of the lattice response with bond breakage, independently from its size. These are the variables that should characterize the continuum point response, those which should enter in a continuum formulation, whatever the phenomenological details or the continuum model chosen (see e.g. Reference [20]).

In the mechanical problem, we characterize the distribution of local currents with the evolution of the lattice degradation (bond failures). For this, we introduce the moments which are calculated according to the formula:

$$M_m = \int i^m N(i)\,\mathrm{d}i \tag{3}$$

where i is the current of each bond, $N(i)$ is the number of bonds whose current is in the range of $[i, i + \mathrm{d}i]$, and m is the order of moment. We limit the analysis to moments of order up to 4. This assumption is equivalent to a truncature in a series. The zero-order moment is the number of unbroken bonds, the first-order moment is proportional to the average value of the current. The

second-order moment is proportional to the overall conductance $\bar{G}$ of the lattice (stiffness in the mechanical problem):

$$M_2 = \int ri^2 N(i)\,\mathrm{d}i = 2\bar{G}v^2 = 2\bar{G} \tag{4}$$

where r is the local resistance of the bond (unit resistance here) and v is the voltage difference applied to the lattice, equal to one in our case. Note that the fourth-order moment is a measure of the dispersion of conductance.

As each lattice has a unique distribution of bond thresholds, several computations with different random seeds following a uniform distribution must be performed in order to have a representative statistical treatment of the results for which useful conclusions about the average behaviour of the lattice can be made. Figure 5 represents the average moments of 300 different random seeds for different lattice sizes as a function of the moment of order 2 until the peak current. In these diagrams, and in all further similar curves in the paper, every curve represents, in a logarithmic scale, the opposite of the moment of order i M_i, divided by its value at the beginning of the calculation M_i^0 (no damage). Hence, the zero-order moment increases as the number of unbroken bonds decreases and the second-order moment increases as the overall conductance decreases. We can observe that until the peak, the curves of M_0, M_1 and M_2 versus M_2 are independent from the size of the lattice approximately. It indicates that the average conductance is a parameter which describes the distribution of current and its evolution due to bond breakage, whatever the size of the lattice. It means also that the overall degradation of conductance (stiffness) is the parameter which represents local bond breakage in the continuum approach. This is consistent with what was observed by Delaplace *et al.* [17], with lattices ranging from size 8 to 64, with a limited number of runs (30) for the larger lattice. It was also shown that the number of broken bonds (e.g. the micro-crack density in a continuum model) could not characterize the state of damage in a size-independent way. Here, each data set for one

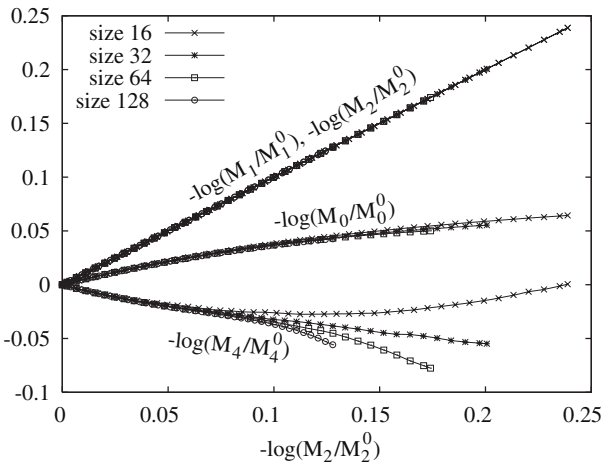

Figure 5. Opposite of the logarithm of the ratio of the moments of order 0,1,2 and 4 to their initial values at the beginning of the computation, as a function of the opposite of the logarithm of moment of order 2 in the mechanical problem for lattice sizes ranging from 16 to 128.

lattice size is comprised of 300 runs and lattices of size 128 could be computed too. For the curves of the moment of order 4, there is aberrance from the size independence according to M_2. This can be explained by the large sensitivity of the higher order moments on small lattices. As the size of the lattice increases, we observe in Figure 5 that the different curves for the fourth-order moment are getting closer and closer. Still, for values of $-\log(M_2/M_2^0)$ less than 0.1, the collapse of the curves onto a single one that is lattice size independent is very good.

3. LATTICE MODEL FOR THE HYDRO-MECHANICAL PROBLEM

In order to represent the influence of material damage on the permeability, it is reasonable to assume that when a bond fails in the mechanical lattice, it opens a larger path for fluid flow in the perpendicular direction (we do not consider here mechanical damage due to hydraulic pressure). This basic scheme is depicted in Figure 6. The hydraulic lattice is built following this principle, with bonds that are perpendicular to the mechanical lattice. The periodicity of the mechanical lattice (Figure 1(b)) yields the hydraulic dual lattice shown in Figure 7 called the sister lattice (to the mechanical one). As mentioned by Dormieux and Kondo [14], the fluid flow at the micro-scale level (bond level) can be described by Darcy equation:

$$q = K \cdot \nabla p \tag{5}$$

where q is the flow rate, ∇p is the drop of pressure p, and k is the local permeability. We are going to assume that when a bond fails, the local permeability in the perpendicular direction is increased by an amplification factor k which is very large, typically of the order of 10^6.

Again, periodic boundary conditions are applied to the hydraulic lattice and we use an electrical analogy. This means that the voltage represents the pressure p, the current represents the flow rate q and the conductance represents the permeability K. A constant drop of pressure equal to 1 is applied at the vertical boundaries of the lattice. The analysis follows the same steps as for the mechanical one. At each step of damage in the mechanical lattice, the flow rate is computed in the sister hydraulic lattice and the various moments of its distribution are computed too. The influence of the value of the amplification factor k on the calculation of the overall permeability (second-order moment in the hydraulic problem) is shown in Figure 8 for

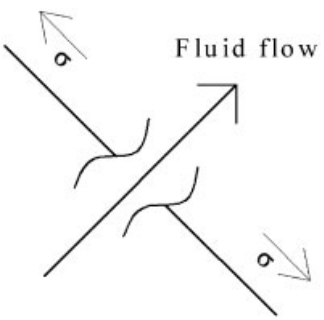

Figure 6. Basic scheme for the coupled hydro-mechanical lattice analysis. When a mechanical bond fails, the permeability of a perpendicular bond increases suddenly.

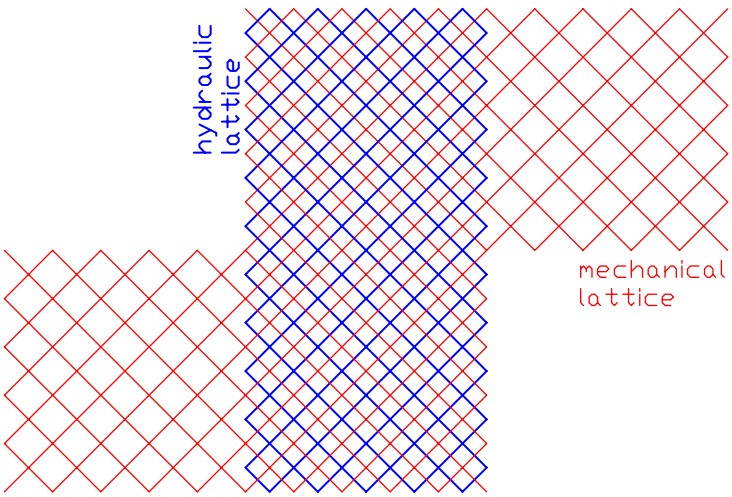

Figure 7. The mechanical and the hydraulic lattices.

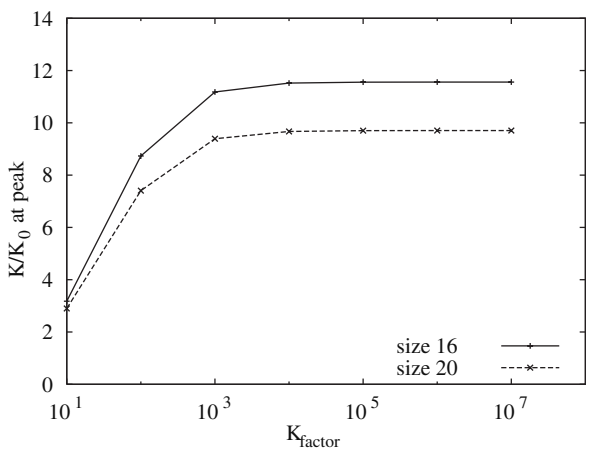

Figure 8. The evolution of the relative average permeability at the peak versus the local amplification of permeability upon bond breakage (K_{factor}).

two sizes of lattice. We can see that for values of k that are higher than of 10^6, this parameter does not play any role on the value of the global permeability.

It is worthwhile to point out that in these lattice analyses, the hydro-mechanical effect is introduced at the local scale, same as the degradation process in the mechanical problem. Furthermore, we analyse here the permeability of the unloaded material. Same as in classical poro-mechanics, there is no effect of the applied stress on the permeability in the reversible regime and it cannot be expected to be observed in the present computations. What we intend to see is on which parameter of the mechanical problem the variation of permeability depends upon material damage growth, and by which moment of the hydraulic and mechanical

problems the evolution of the fluid flow distribution in the lattice can be described in a size-independent way.

3.1. Analysis of the hydraulic problem

We may consider first the distribution of fluid flow in the hydraulic lattice. Figure 9 shows the evolution of the moments of order 0, 1, 2, and 4 as a function of the moment of order 0. This moment is the number of unbroken bonds in the mechanical lattice, or the number of bonds in which the permeability is very small in the hydraulic lattice. We see that for each moment, the curves are far from being independent of the lattice size. The plot of the moments as a function of the second order one (average permeability) in Figure 10 exhibits a much better result (with M_4 there is again aberrance, same as in the mechanical problem, for the same reason). The evolution of the other moments is almost independent of the lattice size, at least for moderate values of the second-order moment ($-\log(M_2/M_2^0) < 0.3$). This result may indeed be easily expected as the hydraulic problem has the same features as the mechanical one.

3.2. Coupling between the two problems

We look now for the variable in the mechanical problem that describes the distribution of the flow rates in the hydraulic problem, independently from the size of the hydraulic sister lattice. Following the same technique as in the mechanical problem, we look at the moments of the distribution of the hydraulic flow rate, and we try to find for which moment of the distribution of the local stress (current) the plots collapse on the same curve for different sizes.

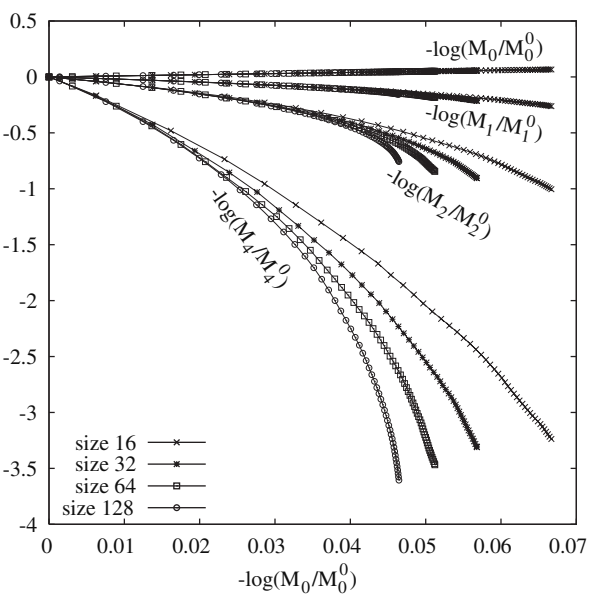

Figure 9. Opposite of the logarithm of the ratio of the moments of order 0, 1, 2 and 4 to their initial values at the beginning of the computation versus opposite of the logarithm of the moment of order zero in the hydraulic problem for lattice sizes ranging from 16 to 128.

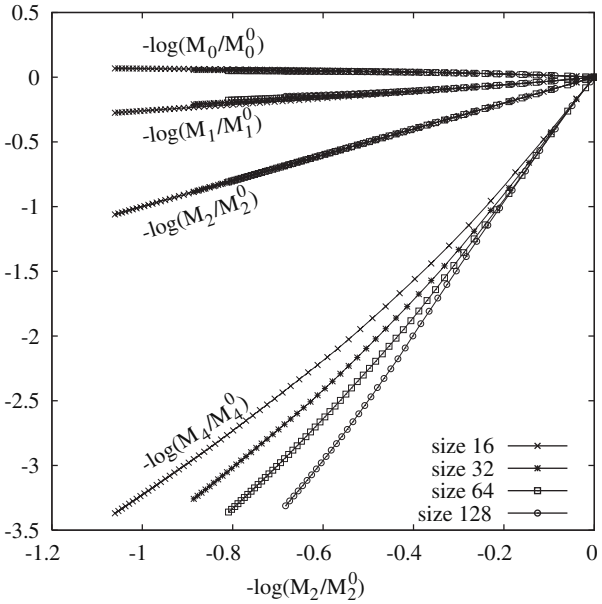

Figure 10. Opposite of the logarithm of the ratio of the moments of order 0, 1, 2 and 4 to their initial values at the beginning of the computation versus opposite of the logarithm of the moment of order 2 in the hydraulic problem, for lattice sizes ranging from 16 to 128.

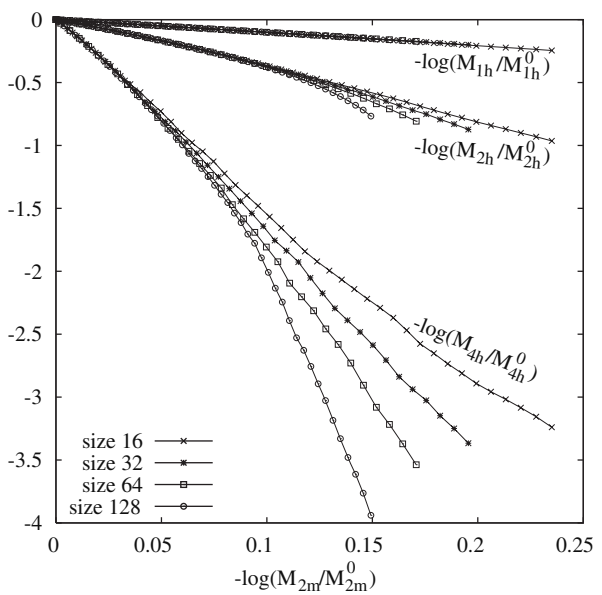

Figure 11. Opposite of the logarithm of the ratio of the moments of order 1, 2 and 4 to their initial values at the beginning of the computation, in the hydraulic problem, as a function of the opposite of the logarithm of the moment of order 2 in the mechanical problem for lattice sizes ranging from 16 to 128.

In Figure 9, the evolution of the moment of order 2 in the hydraulic problem as a function of the moment of order 0 (number of unbroken bonds) is shown. We can see that the curves are not size independent, which means that the moment of order 0 (local degradation) cannot describe the evolution of the overall permeability of the lattice with bond breakage in a unique way for all sizes.

The second-order moment in the mechanical problem is a natural candidate since it is this one which describes the evolution of mechanical damage. Figure 11 shows the plot of the moments of order 1, 2 and 4 in the hydraulic lattice as a function of the moment of order 2 in the mechanical lattice. The collapse of the evolution of the moments of order 1 and 2 for lattice sizes ranging from 16 to 128 is quite satisfactory when $-\log(M_2/M_2^0)$ for the mechanical problem is less than 0.1 (same as in Figure 5). A discrepancy is found for the moment of order 4 (same as in Figure 5, for the same reasons). We have not plotted the moment of order 0 in this figure because it is the same as in the mechanical problem (number of unbroken bonds) and the result for various lattice sizes is the same as in Figure 5 with a good collapse onto a single curve.

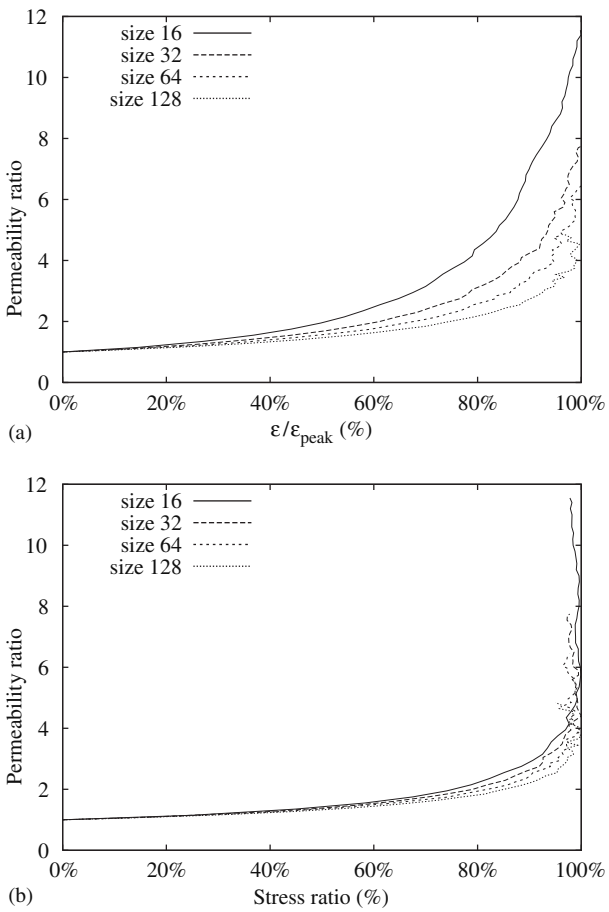

Figure 12. Permeability divided by the initial permeability versus strain (a) and stress (b) ratios up to the peak for various lattice sizes.

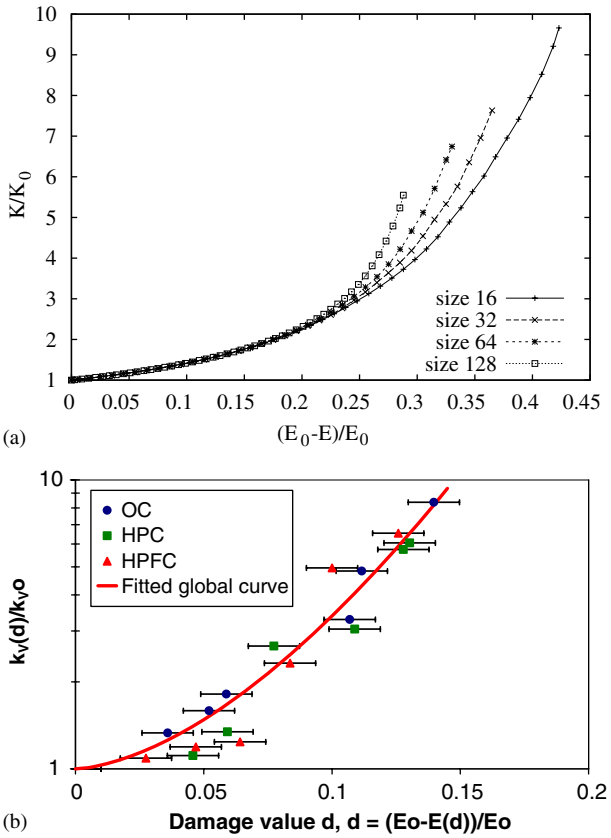

Figure 13. Permeability versus Young Modulus reduction: (a) lattice analysis; and (b) experimental data from Picandet *et al*. [19].

We may conclude that the distribution of the local flow rates due to mechanical bond failures (in the unloaded material) is described by the variation of stiffness due to the mechanical degradation in the mechanical problem, whatever the lattice size when the amount of damage is moderate (moment of order 2 ranging from 0 to 0.1 approximately). In this regime and in the limit of a continuum model, for an infinite lattice size, the variation of material permeability due to bond breakage (micro-cracks) should be controlled by the degradation of stiffness in the mechanical problem, and not by the number of broken bonds (local degradation), the overall strain or the average stress. Figure 12 shows the plots of the evolution of the average permeability divided by the initial permeability (derived from the moment of order 2 in the hydraulic problem), as a function of the applied strain or the applied stress in the mechanical problem. These quantities should be seen here as history variables: the curves show the evolution the average permeability as a function of the maximum strain (stress) reached during the loading history. We can see that for each size of lattice a different curve is obtained. By comparison, Figure 13(a) shows the evolution of the permeability as a function of the evolution of stiffness in the mechanical lattice. For all the sizes considered, the plots collapse onto the

same curve for stiffness variations ranging from 0 to 0.2 approximately, before the peak load. For large variations of the stiffness, lattices have entered far in the softening regime and as seen in Figure 4, the lattice size starts to play an important role because it controls the spacing between the macro-cracks. Therefore, results cannot be interpreted properly in this regime.

Figure 13(b) shows experimental results obtained by Picandet *et al.* [19] for different materials. The gas permeability of circular discs taken from compression cylinders, loaded at different stresses in the pre-peak regime, was obtained after the specimens were dried. Qualitatively, the experimental curves and the lattice analysis provide the same result. Experimentally, the evolution of the permeability with the applied stress (or strain) depends upon the type of material tested. The fact that the variation of permeability with damage recorded experimentally does not depend on the type of concrete tested (ordinary concrete—OC, high performance concrete—HPC, high performance fibre reinforced concrete—HPFC) tends to demonstrate that there is an intrinsic relationship between the permeability and the evolution of the material stiffness indexed by a damage variable. The same type of relationship is recovered from the lattice analysis theoretically, in the regime of moderate micro-cracking.

4. CONCLUSIONS

In this paper, we have studied the mechanical and the hydro-mechanical responses of quasi-brittle materials, focusing in concrete, using a lattice model. In the mechanical problem, the influence of material degradation (bond breakage) is described by the evolution of the material stiffness of the lattice. The result is similar to what was obtained by Delaplace *et al.* [17]. Here lattice sizes range from 16 to 128, with 300 runs for each size. Such a span of sizes could not be achieved in the original study.

The hydro-mechanical problem is analysed by construction of a sister lattice to the mechanical one. When a bond breaks in the mechanical lattice, it increases the permeability of a bond in the hydraulic lattice that is perpendicular to the first one. The analysis of the lattice results follows the technique implemented in the mechanical problem. The various moments of the flow rate distribution are computed and we look for the variable that describes the evolution of these moments independently from the size of the lattice. If such a quantity is found, it is the quantity that describes the evolution of the flow rate distribution with material degradation.

The permeability of the lattice increases progressively with the increase of material degradation. The average permeability constructs lattice size-independent relations with the hydraulic moments of order up to 4, for a moderate material degradation, before the peak load is reached. Finally, the combination of the mechanical and hydraulic analyses was examined. The compliance versus hydraulic moment curves are lattice size independent and consequently the plot of the permeability versus the evolution of damage exhibits the same property. This is consistent with experimental data on various types of concrete. It indicates that in continuum poro-mechanics, the material permeability should be related to the degradation of stiffness. It underlines also the need for a proper description the material stiffness degradation whenever hydro-mechanical problems are considered [23].

ACKNOWLEDGEMENTS

Financial supports from the network on Degradation and Instabilities in Geomaterials with Application to Hazards Mitigation (DIGA), contract HPRN-CT-2002-00220 with the European Commission, and from EDF to the R&DO group are gratefully acknowledged.

REFERENCES

1. Mazars J, Pijaudier-Cabot G. Continuum damage theory: application to concrete. *Journal of Engineering Mechanics* (ASCE) 1989; **115**(2):345–365.
2. Pijaudier-Cabot G, Jason L. Continuum damage modelling and some computational issues. *Revue française de genie civil* 2002; **6**(6):991–1017.
3. Kermani A. Permeability of stressed concrete. *Building Research and Information* 1991; **19**(6):360–366.
4. Hearn N. Effect of shrinkage and load-induced cracking on water permeability of concrete. *ACI Materials Journal* 1999; **96**(2):234–241.
5. Sugiyama T, Bremner TV, Holm TA. Effect of stress on gas permeability in concrete. *ACI Materials Journal* 1996; **93**(5):443–450.
6. Wang K, Jansen DC, Shah SP, Karr AF. Permeability study of cracked concrete. *Cement and Concrete Research* 1997; **27**(3):381–393.
7. Biot MA. General theory of three-dimensional consolidation. *Journal of Applied Physics* 1941; **12**:155–165.
8. Coussy O. *Mechanics of Porous Continua*. Wiley Interscience: New York, 1995.
9. Bary B, Bournazel JP, Bourdarot E. Poro-damage approach applied to hydro-mechanical fracture analysis of concrete. *Journal of Engineering Mechanics* (ASCE) 2000; **126**:937–943.
10. Ulm FJ, Coussy O. Strength growth as chemo-plastic hardening in early age concrete. *Journal of Engineering Mechanics* (ASCE) 1996; **122**:1123–1132.
11. Ulm FJ, Torrenti JM, Adenot F. Chemoporoplasticity of calcium leaching in concrete. *Journal of Engineering Mechanics* (ASCE) 1999; **125**:1200–1211.
12. Bangert F, Grasberger S, Kuhl D, Meschke G. Environmentally induced deterioration in concrete: physical motivations and numerical modeling. *Engineering Fracture Mechanics* 2003; **70**:891–910.
13. Dormieux L, Lemarchand E. Homogenization approach of advection and diffusion in cracked porous materials. *Journal of Engineering Mechanics* (ASCE) 2001; **127**:1267–1274.
14. Dormieux L, Kondo D. Approche micromécanique du couplage perméabilité endommagement. *Comptes Rendus Mécanique* 2004; **332**:135–140.
15. Herrmann HJ, Hansen A, Roux S. Fracture of disordered, elastic lattices in two dimensions. *Physical Reviews B* 1989; **39**:637–648.
16. Hansen A, Roux S, Herrmann HJ. Rupture of central-force lattices. *Journal de Physique* 1989; **50**:733–744.
17. Delaplace A, Pijaudier-Cabot G, Roux S. Progressive damage in discrete models and consequences on continuum modeling. *Journal of Mechanics and Physics of Solids* 1996; **44**(1):99–136.
18. Krajcinovic D, Basista M. Rupture of central force lattices revisited. *Journal de Physique* 1991; **1**:241–245.
19. Picandet V, Khelidj A, Bastian G. Effect of axial compressive damage on gas permeability of ordinary and high-performance concrete. *Cement and Concrete Research* 2001; **31**:1525–1532.
20. Krajcinovic D, Van Mier JGM. Damage and fracture of disordered materials. *CISM Courses and Lectures No. 410*, 2000.
21. De Arcangelis L, Herrmann HJ. Scaling and multiscaling laws in random fuse networks. *Physical Reviews B* 1989; **39**(4):2678–2684.
22. Press WH, Teukolsky SA, Vetterling WT, Flannery BP. *Numerical Recipes in FORTRAN 77*: *The Art of Scientific Computing*. Cambridge University Press: Cambridge, 1992.
23. Jason L, Huerta A, Pijaudier-Cabot G, Ghavamian S. An elastic plastic damage formulation for concrete: application to elementary tests and comparison with an isotropic damage model. *Computer Methods in Applied Mechanics and Engineering* 2005, in press.